

Contribution from the Department of Chemistry, Thimann Laboratories, University of California, Santa Cruz, California 95064, and Department of Chemistry and Biochemistry, University of Windsor, Windsor, Ontario, Canada N9B 3P4

New Octahedral Thiolato Complexes of Divalent Nickel: Syntheses, Structures, and Properties of $(Et_4N)[Ni(SC_5H_4N)_3]$ and $(Ph_4P)[Ni(SC_4H_3N_2)_3] \cdot CH_3CN$

Steven G. Rosenfield, Hilde P. Berends,[†] Lucio Gelmini,[†] Douglas W. Stephan,[†] and Pradip K. Mascharak*

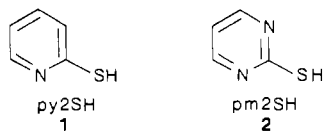
Received January 23, 1987

In aprotic solvents, reactions of $[NiCl_4]^{2-}$ with preformed or generated in situ thiolates from pyridine-2-thiol (py2SH) and pyrimidine-2-thiol (pm2SH) afford the distorted octahedral thiolato complexes $[Ni(S2py)_3]^-$ and $[Ni(S2pm)_3]^-$, respectively. $(Et_4N)[Ni(S2py)_3]$ (**3**) crystallizes in the monoclinic space group $P2_1/c$ with $a = 18.958$ (5) Å, $b = 9.311$ (3) Å, $c = 15.090$ (4) Å, $\beta = 104.91$ (2)°, $V = 2574$ (1) Å³, and $Z = 4$. The structure of **3** was refined to $R = 4.68\%$ on the basis of 2636 unique ($F_o^2 > 3\sigma(F_o^2)$) data. $(Ph_4P)[Ni(S2pm)_3] \cdot CH_3CN$ (**4b**) also crystallizes in the monoclinic space group $P2_1/c$ with $a = 18.002$ (7) Å, $b = 9.951$ (4) Å, $c = 22.791$ (1) Å, $\beta = 112.27$ (3)°, $V = 3778$ (3) Å³, and $Z = 4$. On the basis of 2565 unique data, the structure of **4b** was refined to $R = 4.66\%$. These discrete thiolato complexes of nickel(II) contain three four-membered N,S-chelate rings with exceptionally small N-Ni-S "bite" angles of ca. 67°. The average Ni(II)-N and Ni(II)-S_{th} (th = thiolate) distances are 2.052 (4) and 2.528 (1) Å (in **3**) and 2.043 (5) and 2.495 (2) Å (in **4b**) respectively. Both complexes are isolated as the *mer* isomer. Various spectroscopic studies show that pm2S⁻ is the stronger ligand and gives rise to a nickel(II) complex that is more resistant to oxidation. The three complexes reported in this paper belong to a relatively scarce class of octahedral nickel(II) thiolates. Unlike the tetrahedral thiolato complexes $[Ni(SAr)_4]^{2-}$, these octahedral species are quite stable in presence of protic solvents like alcohols.

Introduction

The discovery of a low-potential S-ligated nickel center at the active site of several hydrogenases¹⁻⁷ has initiated synthetic attempts toward isolation of discrete mononuclear thiolato complexes of nickel.⁸⁻¹⁰ Analysis of EPR spectra indicated that nickel is in a rhombically distorted octahedral coordination sphere in these proteins.^{3,4,6} Recent EXAFS studies also support a tetragonally distorted octahedral or square-pyramidal geometry around nickel.¹¹ Although the EXAFS data can be explained by assuming only Ni-S interactions, the presence of a smaller number of low atomic number scatterers in the first coordination shell of nickel is not completely ruled out. Indeed, EPR studies of Ni(III) complexes (generated in situ) of peptides containing sulfhydryl groups strongly suggest that the Ni(III) center of the enzyme(s) contains one cysteine S atom as equatorial donor and two cysteine S atoms as axial donors in a tetragonal geometry.¹² The other coordination positions could be occupied by histidine and/or amido N atoms.¹³

The mononuclear thiolato complexes of nickel reported so far are distorted tetrahedral. Recently, we have reported the convenient synthesis and properties of arenethiolates of the type $[Ni(SAr)_4]^{2-}$.¹⁰ The corresponding alkanethiolates $[Ni(SR)_4]^{2-}$, R = alkyl have not been synthesized.¹⁴ Examples of octahedral nickel complexes containing thiolato ligands are however, scarce. To date, the structure of only one such complex has been determined; in *cis*-bis(2,2'-bipyridine)bis(benzenethiolato)nickel(II) dideuteriohydrate,¹⁵ two thiophenolate anions occupy *cis* positions in the equatorial plane of nickel. In this paper, we report the syntheses, structures, and spectral characteristics of three octahedral nickel(II) thiolato complexes derived from pyridine-2-thiol(py2SH) (**1**) and pyrimidine-2-thiol (pm2SH) (**2**), respectively. As in the iron complexes,^{16,17} these two ligands give rise to three four-membered S,N-chelate rings.



Experimental Section

Preparation of Compounds. Pyridine-2-thiol and pyrimidine-2-thiol were procured from Aldrich Chemical Co. and used without further purification. $(Et_4N)_2NiCl_4$ was synthesized by following a standard procedure.¹⁸ In the following preparations, degassed solvents were used and all manipulations were performed under an atmosphere of dry and pure dinitrogen.

$(Et_4N)[Ni(SC_5H_4N)_3]$ (**3**). A solution of sodium methoxide was prepared by dissolving 0.40 g (17.5 mmol) of sodium in 35 mL of methanol. A 1.93-g (17.5-mmol) sample of pyridine-2-thiol (py2SH) was added to the methoxide solution followed by the addition of an equivalent amount (3.7 g) of Et_4NBr . After 1 h of stirring, the solvent was removed in vacuo. The oily residue was extracted with 30 mL of acetonitrile, and the extract was filtered. To the filtrate, containing tetraethylammonium

- (1) Thomson, A. J. *Nature (London)* **1982**, *298*, 602.
- (2) (a) Graf, E.; Thauer, R. K. *FEBS Lett.* **1981**, *136*, 165. (b) Albracht, S. P. J.; Graf, E.-G.; Thauer, R. K. *FEBS Lett.* **1982**, *140*, 311. (c) Kojima, N.; Fox, J. A.; Hausinger, R. P.; Daniels, L.; Orme-Johnson, W. H.; Walsh, C. *Proc. Natl. Acad. Sci. U.S.A.* **1983**, *80*, 378.
- (3) Lancaster, J. R. Jr., *Science (Washington, D.C.)* **1982**, *216*, 1324.
- (4) Kruger, H.-J.; Huynh, B. H.; Ljungdahl, P. O.; Xavier, A. V.; DerVartanian, D. V.; Moura, I.; Peck, H. D., Jr.; Teixeira, M.; Moura, J. J. G.; LeGall, J. *J. Biol. Chem.* **1982**, *257*, 14620.
- (5) Udden, G.; Bocher, R.; Knecht, J.; Kroger, A. *FEBS Lett.* **1982**, *145*, 230.
- (6) (a) Cammack, R.; Patil, D.; Aguirre, R.; Hatchikian, E. C. *FEBS Lett.* **1982**, *142*, 289. (b) LeGall, J.; Ljungdahl, P. O.; Moura, I.; Peck, H. D. Jr.; Xavier, A. V.; Moura, J. J. G.; Teixeira, M.; Huynh, B. H.; DerVartanian, D. V. *Biochem. Biophys. Res. Commun.* **1982**, *106*, 610. (c) Moura, J. J. G.; Moura, I.; Huynh, B. H.; Kruger, H.-J.; Teixeira, M.; DuVarney, R. C.; DerVartanian, D. V.; Xavier, A. V.; Peck, H. D., Jr.; LeGall, J. *Biochem. Biophys. Res. Commun.* **1982**, *108*, 1388. (d) Teixeira, M.; Moura, I.; Xavier, A. V.; DerVartanian, D. V.; LeGall, J.; Peck, H. D., Jr.; Huynh, B. H.; Moura, J. J. G. *Eur. J. Biochem.* **1983**, *130*, 481.
- (7) Albracht, S. P. J.; Albracht-Ellmer, K. J.; Schmedding, D. J. M.; Slater, E. C. *Biochim. Biophys. Acta* **1982**, *681*, 330.
- (8) (a) Holah, D. G.; Coucouvanis, D. *J. Am. Chem. Soc.* **1975**, *97*, 6917. (b) Swenson, D.; Baenziger, N. C.; Coucouvanis, D. *J. Am. Chem. Soc.* **1978**, *100*, 1932. (c) Coucouvanis, D.; Swenson, D.; Baenziger, N. C.; Murphy, C.; Holah, D. G.; Sfaras, N.; Simopoulos, A.; Kostikas, A. *J. Am. Chem. Soc.* **1981**, *103*, 3350.
- (9) Yamamura, T.; Miyamae, H.; Katayama, Y.; Sasaki, Y. *Chem. Lett.* **1985**, 269.
- (10) Rosenfield, S. G.; Armstrong, W. H.; Mascharak, P. K. *Inorg. Chem.* **1986**, *25*, 3014.
- (11) (a) Lindahl, P. A.; Kojima, N.; Hausinger, R. P.; Fox, J. A.; Teo, B.-K.; Walsh, C. T.; Orme-Johnson, W. H. *J. Am. Chem. Soc.* **1984**, *106*, 3062. (b) Scott, R. A.; Wallin, S. A.; Czechowski, M.; DerVartanian, D. V.; LeGall, J.; Peck, H. D., Jr.; Moura, I. *J. Am. Chem. Soc.* **1984**, *106*, 6864.
- (12) Sugiura, Y.; Kuwahara, J.; Suzuki, T. *Biochem. Biophys. Res. Commun.* **1983**, *115*, 878.
- (13) (a) Fabbri, L.; Perotti, A.; Poggi, A. *Inorg. Chem.* **1983**, *22*, 1411. (b) Jacobs, S. A.; Margerum, D. W. *Inorg. Chem.* **1984**, *23*, 1195 and references therein.
- (14) Watson, A. D.; Rao, C. P.; Dorfman, J. R.; Holm, R. H. *Inorg. Chem.* **1985**, *24*, 2820.
- (15) Osakada, K.; Yamamoto, T.; Yamamoto, A.; Takenaka, A.; Sasada, Y. *Acta Crystallogr., Sect. C: Cryst. Struct. Commun.* **1984**, *C40*, 85.
- (16) Rosenfield, S. G.; Swedberg, S. A.; Arora, S. K.; Mascharak, P. K. *Inorg. Chem.* **1986**, *25*, 2109.
- (17) (a) Rosenfield, S. G.; Arora, S. K.; Mascharak, P. K. *Inorg. Chim. Acta*, in press. (b) Latham, I. A.; Leigh, G. J.; Pickett, C. J.; Huttner, G.; Jibrill, I.; Zubieta, J. *J. Chem. Soc., Dalton Trans.* **1986**, 1181.
- (18) Gill, N. S.; Taylor, F. B. *Inorg. Synth.* **1967**, *9*, 136.

* To whom correspondence should be addressed at the University of California.

[†] University of Windsor.

pyridine-2-thiolate, was slowly added with stirring a solution of 2.0 g (4.35 mmol) of $(Et_4N)_2NiCl_4$ in ~80 mL of acetonitrile. As the addition of the nickel salt continued, the color changed from the initial pale yellow to milky green. A transient gold-colored precipitate was observed during the last part of mixing. After the mixture was stirred for another hour, the volume of the milky green mixture was reduced to ~45 mL and it was stored at 0 °C for 2 h. Next, the mixture was filtered, and the clear green filtrate was kept at -20 °C for 14 h when green crystals separated. These crystals were collected by filtration and recrystallized from 40 mL of 1:6 v/v acetonitrile/diethyl ether. A 1.37 g (61%) yield of large green blocks was obtained; mp 187 °C dec. Anal. Calcd for $C_{23}H_{32}N_4NiS_3$: C, 53.16; H, 6.21; N, 10.79; Ni, 11.31. Found: C, 53.23; H, 6.27; N, 10.86; Ni, 11.27. Selected IR bands (KBr pellet, cm^{-1}): 1580 (s), 1550 (m), 1440 (s), 1420 (vs), 1270 (m), 1150 (s), 1005 (m), 760 (s), 735 (s), 500 (m), 460 (m), 420 (w).

$(Et_4N)[Ni(SC_4H_3N_2)_3]$ (**4a**). A 1.60-g (14-mmol) sample of solid pyrimidine-2-thiol (pm2SH) was added to a solution of 2.0 g (4.35 mmol) of $(Et_4N)_2NiCl_4$ in 70 mL of acetonitrile. The initial blue color changed to bluish green as part of the thiol dissolved. The major portion of the added thiol, however, remained insoluble. Next, a solution of 3 mL (21.5 mmol) of triethylamine in 10 mL of acetonitrile was slowly added to the bluish green slurry with constant stirring. As the addition of triethylamine progressed, the color of the mixture changed from milky green to brown, and then a heavy golden brown precipitate appeared. The precipitate dissolved as the addition continued and finally a dark green solution containing small amount of white precipitate resulted. After 1 h of stirring the mixture was filtered. The volume of the clear green filtrate was reduced to ~40 mL, and it was kept at 0 °C for 4 h. A batch of clear crystals was obtained. The IR spectrum showed that this material is Et_3NHCl . After the crystals of Et_3NHCl were removed by filtration, the green filtrate was stored at -20 °C for 18 h when a mixture of dark green and clear crystals separated. Recrystallization of this mixture from 40 mL of acetonitrile afforded 0.95 g (42%) of pure product as dark green needles, mp 195 °C dec. Anal. Calcd for $C_{20}H_{29}N_7NiS_3$: C, 45.96; H, 5.60; N, 18.78; Ni, 11.24. Found: C, 45.86; H, 5.64; N, 18.82; Ni, 11.14. Selected IR bands (KBr pellet, cm^{-1}): 1570 (s), 1550 (s), 1370 (vs), 1250 (m), 1200 (m), 1000 (m), 770 (m), 750 (m), 650 (w), 470 (m).

The above-mentioned method was also used to synthesize **3** in 60% yield.

Since crystals of **4a** were not suitable for structure determination by X-ray crystallography, we isolated the Ph_4P^+ salt of the $[Ni(SC_4H_3N_2)_3]^-$ anion.

$(Ph_4P)[Ni(SC_4H_3N_2)_3] \cdot CH_3CN$ (**4b**). This complex was synthesized from $(Ph_4P)_2NiCl_4$ following the procedure described above. The crude product was recrystallized from 40 mL of hot (~65 °C) acetonitrile. The yield was 65% (2.1 g); mp 155 °C dec. Anal. Calcd for $C_{38}H_{32}N_7NiPS_3$: C, 59.06; H, 4.18; N, 12.70; Ni, 7.60. Found: C, 59.11; H, 4.21; N, 12.74; Ni, 7.87. Selected IR bands (KBr pellet, cm^{-1}): 1570 (m), 1540 (m), 1380 (m), 1240 (m), 1200 (m), 1000 (w), 770 (w), 750 (m), 730 (m), 690 (m), 650 (w), 530 (s), 470 (w).

X-ray Data Collection and Reduction. Green crystals of **3** were obtained by slow diffusion of diethyl ether into an acetonitrile solution. Green blocks of **4b** were isolated by slow cooling of an acetonitrile solution. Diffraction experiments were performed on a four-circle Syntex $P2_1$ diffractometer with graphite-monochromatized Mo $K\alpha$ radiation. The initial orientation matrices were obtained from 15 machine-centered reflections selected from rotation photographs. These data were used to determine the crystal systems. Partial rotation photographs around each axis were consistent with monoclinic crystal systems. Ultimately, 30 high-angle reflections ($22^\circ < 2\theta < 25^\circ$) were used to obtain the final lattice parameters and the orientation matrix for **3**. For **4b**, 60 such reflections were employed. Machine parameters, crystal data, and data collection parameters are summarized in Table I. The observed extinctions were consistent with the space group $P2_1/c$ for both compounds. $\pm h, +k, +l$ data were collected in one shell. For **3**, the data were collected over the range $4.5^\circ < 2\theta < 45.0^\circ$, while for **4b**, the range was $4.5^\circ < 2\theta < 40.0^\circ$. Three standard reflections were recorded every 197 reflections in both cases. Their intensities showed no statistically significant change over the entire period of data collection. The data were processed by using the SHELX-76 program package.¹⁹ The total number of reflections with $F_o^2 > 3\sigma(F_o^2)$ used in the refinement procedure are given in Table I. Since the absorption coefficients are small (for **3**, $\mu = 9.52 \text{ cm}^{-1}$; for **4b**, $\mu = 7.02 \text{ cm}^{-1}$), absorption corrections were not applied to either data set.

Solutions and Refinements of the Structures. Scattering factors for the non-hydrogen atoms were taken from the literature tabulations.²⁹ The

Table I. Summary of Crystal Data, Intensity Collection, and Structure Refinement Parameters for $(Et_4N)[Ni(SC_4H_3N_2)_3]$ (**3**) and $(Ph_4P)[Ni(SC_4H_3N_2)_3] \cdot CH_3CN$ (**4b**)

	3	4b
formula (mol wt)	$C_{23}H_{32}N_4NiS_3$ (519.15)	$C_{38}H_{32}N_7NiPS_3$ (772.13)
cryst color and form	green blocks	green blocks
<i>a</i> , Å	18.958 (5)	18.002 (7)
<i>b</i> , Å	9.311 (3)	9.951 (4)
<i>c</i> , Å	15.090 (4)	22.791 (1)
β , deg	104.91 (2)	112.27 (3)
cryst syst	monoclinic	monoclinic
space group	$P2_1/c$	$P2_1/c$
vol, Å ³	2574 (1)	3778 (3)
<i>d</i> _{calcd} ^a , g/cm ³	1.34	1.36
<i>d</i> _{obsd} ^a , g/cm ³	1.33	1.35
<i>Z</i>	4	4
cryst dimens, mm	0.67 × 0.53 × 0.45	0.46 × 0.46 × 0.77
abs coeff μ , cm ⁻¹	9.52	7.02
radiation (λ , Å)	Mo $K\alpha$ (0.710 69)	Mo $K\alpha$ (0.710 69)
temp, °C	24	24
scan speed, deg/min	2.0–5.0 ($\theta/2\theta$ scan)	2.0–5.0 ($\theta/2\theta$ scan)
scan range, deg	1.0 below $K\alpha_1$, 1.0 above $K\alpha_2$	1.0 below $K\alpha_1$, 1.0 above $K\alpha_2$
bkgd/scan time ratio	0.5	0.5
data colld	3757	3688
no. of unique data ($F_o^2 >$ $3\sigma(F_o^2)$)	2636	2565
no. of variables	165	261
<i>R</i> , %	4.68	4.66
<i>R</i> _w , %	5.46	5.15
max Δ/σ in final cycle	0.008	0.002
largest residual electron density, e/Å ³	0.91	0.39
atom associated with residual density	C21–C25	C45

^aDetermined by flotation in CCl_4 /cyclohexane.

Ni atom position in **3** was determined by the heavy-atom (Patterson) method. The direct methods program (SHELX-76) was employed to obtain the Ni and S atom positions for **4b**. Positions of the remaining non-hydrogen atoms were revealed in subsequent difference Fourier maps. Refinement was carried out by using full-matrix least squares techniques on *F* minimizing the function $\sum w(|F_o| - |F_c|)^2$ where the weight *w* is defined as $4F_o^2/\sigma^2(F_o^2)$ and F_o and F_c are the observed and calculated structure factor amplitudes. In the final cycles of refinement, the Ni, S, N, and P atoms were assigned anisotropic temperature factors. C atoms were described by isotropic temperature factors. Hydrogen atom positions were allowed to ride on the carbon to which they are bonded, assuming a C–H bond length of 0.95 Å. Hydrogen atom temperature factors were fixed at 1.10 times the isotropic temperature factor of the C atom to which they are bonded. In both cases, the hydrogen atom contributions were calculated but not refined. The final values of $R = \sum ||F_o| - |F_c||/\sum |F_o|$ and $R_w = (\sum w(|F_o| - |F_c|)^2/\sum w|F_o|^2)^{1/2}$ are given in Table I. The maximum Δ/σ values on any of the parameters in the final cycles of refinement are also included in Table I. Final difference Fourier map calculations showed no peak of chemical significance in either case. The magnitudes of the largest peaks in the final difference maps and the locations of these residuals are collected in Table I. The following data are tabulated: positional parameters (Table II) and selected bond distances and angles (Table III). Thermal parameters (Table S1), hydrogen atom parameters (Table S2), bond distances and angles associated with the counterions and the acetonitrile molecule (Table S3), and values of $10|F_o|$ and $10|F_c|$ (Table S4) have been deposited as supplementary material.

Other Physical Measurements. The reported melting points are uncorrected. Absorption spectra were obtained either on a Cary model 14 or a Hitachi 100-80 spectrophotometer. ¹H NMR spectra were recorded on a General Electric 300-MHz GN-300 spectrometer. Following the usual convention for the spectra of paramagnetic molecules, we designated chemical shifts that are upfield and downfield of the Me_4Si reference as positive and negative, respectively. Electrochemical measurements were made with standard Princeton Applied Research instrumentation using a Pt or a glassy-carbon working electrode. Infrared spectra were measured on a Nicolet MX-S FTIR spectrometer. Microanalyses were performed by Atlantic Microlab Inc., Atlanta, GA. Nickel was estimated gravimetrically with dimethylglyoxime.

(19) Sheldrick, G. M. "SHELX-76, Program for Crystal Structure Determination"; University of Cambridge: Cambridge, England, 1976.

Table II. Positional Parameters ($\times 10^4$)

atom	x	y	z	atom	x	y	z
Compound 3							
Ni	2490 (1)	667 (1)	1406 (1)	S1	2210 (1)	2587 (1)	421 (1)
S2	3342 (1)	-1264 (1)	912 (1)	S3	2759 (1)	-297 (1)	2685 (1)
N1	3472 (3)	2218 (4)	1612 (2)	N2	1640 (3)	-935 (4)	895 (2)
N3	1575 (3)	1501 (4)	1956 (2)	N4	3023 (3)	-4825 (4)	3561 (2)
C1	3224 (3)	3092 (5)	1027 (2)	C2	3781 (4)	4271 (6)	957 (3)
C3	4574 (4)	4528 (7)	1495 (3)	C4	4818 (4)	3647 (6)	2092 (3)
C5	4259 (3)	2490 (5)	2126 (3)	C11	2221 (3)	-1853 (5)	689 (2)
C12	1879 (4)	-3134 (6)	320 (3)	C13	965 (4)	-3404 (7)	168 (3)
C14	368 (4)	-2458 (6)	363 (3)	C15	746 (4)	-1231 (6)	732 (3)
C21	1829 (4)	813 (6)	2606 (3)	C22	1339 (4)	1041 (7)	3131 (4)
C23	598 (5)	1939 (8)	2967 (4)	C24	333 (5)	2631 (7)	2312 (4)
C25	862 (4)	2384 (6)	1810 (3)	C31	2382 (4)	-3787 (6)	3796 (3)
C32	1474 (4)	-4418 (6)	3845 (3)	C33	2575 (4)	-5443 (5)	2814 (3)
C34	2246 (4)	-4381 (7)	2202 (3)	C35	3887 (4)	-4026 (6)	3518 (3)
C36	4463 (5)	-3470 (7)	4236 (3)	C37	3237 (4)	-6039 (5)	4106 (3)
C38	3923 (4)	-7126 (6)	4000 (3)				
Compound 4b							
Ni	6937 (1)	1898 (1)	1568 (1)	S1	8165 (1)	2446 (2)	2484 (1)
S2	7478 (1)	747 (2)	850 (1)	S3	5906 (1)	2333 (2)	2061 (1)
P	8537 (1)	-1955 (2)	4208 (1)	N1	7338 (3)	3799 (5)	1500 (2)
N2	6090 (3)	1710 (5)	665 (2)	N3	6603 (3)	204 (5)	1896 (2)
N4	8459 (3)	4981 (6)	2232 (3)	N5	6180 (4)	728 (6)	-262 (3)
N6	5646 (3)	-200 (7)	2368 (3)	N7	3934 (5)	621 (8)	5404 (4)
C1	7987 (4)	3876 (7)	2043 (3)	C2	7155 (5)	4829 (8)	1103 (4)
C3	7630 (5)	5978 (9)	1259 (4)	C4	8254 (5)	5987 (9)	1819 (4)
C11	6503 (4)	1069 (7)	362 (3)	C12	5319 (4)	2004 (7)	338 (3)
C13	4948 (5)	1684 (7)	-301 (4)	C14	5413 (5)	1061 (8)	-555 (4)
C21	6048 (4)	645 (6)	2119 (3)	C22	6781 (4)	-1096 (7)	1934 (3)
C23	6398 (4)	-1984 (8)	2188 (3)	C24	5850 (5)	-1492 (8)	2387 (4)
C31	8140 (3)	9639 (6)	4308 (3)	C32	8392 (4)	10250 (6)	4899 (3)
C33	8091 (4)	11502 (7)	4959 (4)	C34	7550 (4)	12144 (7)	4439 (3)
C35	7292 (4)	11532 (7)	3849 (3)	C36	7581 (4)	10278 (6)	3786 (3)
C41	9134 (4)	7372 (6)	4970 (3)	C42	9946 (4)	7734 (7)	5260 (3)
C43	10396 (4)	7250 (7)	5858 (3)	C44	10060 (4)	6471 (7)	6179 (3)
C45	9250 (4)	6149 (7)	5906 (4)	C46	8795 (4)	6583 (6)	5289 (3)
C51	9147 (4)	8220 (6)	3745 (3)	C52	9051 (4)	9292 (8)	3347 (4)
C53	9510 (5)	9364 (9)	2963 (4)	C54	10031 (5)	8364 (8)	2987 (4)
C55	10134 (4)	7324 (8)	3381 (3)	C56	9689 (4)	7214 (7)	3763 (3)
C61	7716 (3)	6932 (6)	3823 (3)	C62	7796 (4)	5866 (6)	3457 (3)
C63	7155 (4)	4972 (7)	3191 (3)	C64	6456 (4)	5169 (7)	3283 (3)
C65	6370 (4)	6209 (6)	3643 (3)	C66	7002 (3)	7093 (6)	3920 (3)
C71	4357 (6)	93 (10)	5831 (5)	C72	4893 (6)	-563 (11)	6382 (5)

Results and Discussion

Two distorted octahedral thiolato complexes of nickel have been isolated from reaction mixtures of $[\text{NiCl}_4]^{2-}$ and the corresponding thiolate in acetonitrile. As discussed earlier,^{9,10} choice of an aprotic solvent like acetonitrile and the right order of addition (nickel to thiolate) allowed formation and successful isolation of discrete thiolato complexes of nickel. In the case of pm2SH, addition of $[\text{NiCl}_4]^{2-}$ to preformed $(\text{Et}_4\text{N})(\text{S}2\text{pm})$ in acetonitrile resulted in precipitation of a brown flocculent solid which did not dissolve on further stirring and/or heating. To avoid this problem with pm2SH, the thiolate anion was generated in situ by addition of triethylamine to a slurry of the thiol in a solution of the nickel salt. The method was also used to synthesize 3. We believe that this method of in situ generation of thiolate in aprotic solvents will prove helpful in syntheses of other thiolato complexes. However, 4a and 4b can be synthesized from preformed $(\text{R}_4\text{N})(\text{S}2\text{pm})$ and $[\text{NiCl}_4]^{2-}$ in DMF without the formation of insoluble polymer(s). IR spectra of 3–4b exhibit no N–H stretch in the 3500–3000- cm^{-1} region, and hence the “thione” form of the ligands has no contribution to the structures of these complexes.^{21,22}

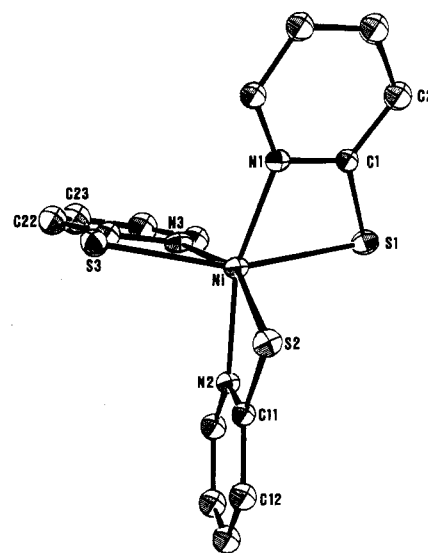


Figure 1. ORTEP drawing of $[\text{Ni}(\text{SC}_5\text{H}_4\text{N})_3]^-$ (anion of 3) showing 30% probability ellipsoids and the atom-labeling scheme. Hydrogen atoms are omitted for clarity.

Structure of $(\text{Et}_4\text{N})[\text{Ni}(\text{SC}_5\text{H}_4\text{N})_3]$ (3). This compound crystallizes in the monoclinic space group $P2_1/c$. The crystal structure consists of discrete cations and anions. Structural features of the cation are unexceptional and are not considered. The structure

- (20) Cromer, D. T.; Waber, J. T. *International Tables for X-ray Crystallography*; Kynoch: Birmingham, England, 1974; Vol. IV.
- (21) (a) Kennedy, P. B.; Lever, A. B. P. *Can. J. Chem.* **1972**, *50*, 3488. (b) Evans, I. P.; Wilkinson, G. *J. Chem. Soc., Dalton Trans.* **1974**, 946.
- (22) (a) Abbot, J.; Goodgame, D. M. L.; Jeeves, I. *J. Chem. Soc., Dalton Trans.* **1978**, 880. (b) Goodgame, D. M. L.; Jeeves, I.; Leach, G. A. *Inorg. Chim. Acta* **1980**, *39*, 247.

Table III. Selected Bond Distances and Angles

Compound 3					
Distances (Å)					
Ni-S1	2.541 (1)	Ni-N1	2.034 (4)	Ni-S2	2.526 (1)
Ni-N2	2.041 (4)	Ni-S3	2.518 (1)	Ni-N3	2.081 (4)
S1-C1	1.725 (5)	S2-C11	1.725 (5)	N1-C1	1.349 (6)
N2-C11	1.352 (6)	C1-C2	1.409 (7)	C11-C12	1.411 (7)
C2-C3	1.379 (8)	C12-C13	1.358 (8)	C3-C4	1.369 (8)
C13-C14	1.376 (8)	C4-C5	1.380 (7)	C14-C15	1.384 (8)
N1-C5	1.353 (6)	N2-C15	1.334 (7)	S3-C21	1.719 (5)
N3-C21	1.354 (6)	C21-C22	1.400 (8)	C22-C23	1.366 (9)
C23-C24	1.365 (9)	C24-C25	1.409 (9)	N3-C25	1.326 (7)
Angles (deg)					
S1-Ni-S2	103.4 (1)	S1-Ni-N1	67.4 (1)	S1-Ni-S3	156.0 (1)
S1-Ni-N2	101.5 (1)	S2-Ni-S3	97.6 (1)	S1-Ni-N3	95.7 (1)
S2-Ni-N1	99.2 (1)	S3-Ni-N1	98.0 (1)	S2-Ni-N2	67.8 (1)
S3-Ni-N2	97.1 (1)	S2-Ni-N3	156.6 (1)	S3-Ni-N3	67.4 (1)
N1-Ni-N2	161.3 (2)	N1-Ni-N3	106.0 (1)	N2-Ni-N3	95.4 (3)
Ni-S1-C1	75.6 (2)	Ni-S2-C11	75.9 (2)	Ni-N1-C1	103.7 (3)
Ni-N2-C11	103.0 (3)	N1-C1-S1	113.2 (4)	N2-C11-S2	113.3 (3)
S1-C1-C2	126.8 (4)	S2-C11-C12	127.0 (4)	N1-C1-C2	121.0 (5)
N2-C11-C12	119.7 (4)	C1-C2-C3	119.4 (5)	C11-C12-C13	118.9 (5)
C2-C3-C4	124.0 (6)	C12-C13-C14	121.6 (6)	C3-C4-C5	117.9 (6)
C13-C14-C15	116.8 (6)	C4-C5-N1	123.1 (5)	C14-C15-N2	123.2 (5)
Ni-S3-C21	77.0 (2)	Ni-N3-C21	102.2 (3)	N3-C21-S3	113.4 (4)
S3-C21-C22	126.7 (4)	N3-C21-C22	119.9 (5)	C21-C22-C23	118.7 (6)
C22-C23-C24	121.9 (7)	C23-C24-C25	116.8 (7)	C24-C25-N3	122.2 (6)
Compound 4b					
Distances (Å)					
Ni-S1	2.460 (2)	Ni-S2	2.480 (2)	Ni-S3	2.545 (2)
Ni-N1	2.051 (5)	Ni-N2	2.053 (5)	Ni-N3	2.025 (5)
S1-C1	1.702 (7)	S2-C11	1.715 (7)	S3-C21	1.697 (7)
P-C31	1.789 (6)	P-C41	1.791 (6)	P-C51	1.797 (6)
P-C61	1.787 (6)	N1-C1	1.344 (8)	N1-C2	1.324 (8)
N2-C11	1.351 (8)	N2-C12	1.334 (8)	N3-C21	1.353 (8)
N3-C22	1.328 (8)	N4-C1	1.356 (8)	N4-C4	1.327 (9)
N5-C11	1.359 (8)	N5-C14	1.328 (9)	N6-C21	1.366 (8)
N6-C24	1.334 (9)	N7-C71	1.11 (1)	C2-C3	1.39 (1)
C3-C4	1.34 (1)	C12-C13	1.390 (9)	C13-C14	1.337 (9)
C22-C23	1.376 (9)	C23-C24	1.33 (1)	C31-C32	1.389 (8)
Angles (deg)					
S1-Ni-S2	102.2 (1)	S1-Ni-S3	99.1 (1)	S2-Ni-S3	154.8 (1)
S1-Ni-N1	68.3 (2)	S2-Ni-N1	98.0 (1)	S3-Ni-N1	102.2 (1)
S1-Ni-N2	163.4 (1)	S2-Ni-N2	68.0 (1)	S3-Ni-N2	94.0 (1)
N1-Ni-N2	99.1 (2)	S1-Ni-N3	99.7 (1)	S2-Ni-N3	96.0 (1)
S3-Ni-N3	67.1 (1)	N1-Ni-N3	163.2 (2)	N2-Ni-N3	94.7 (2)
Ni-S1-C1	77.1 (2)	Ni-S2-C11	77.2 (2)	Ni-S3-S21	75.6 (2)
Ni-N1-C1	101.1 (4)	Ni-N1-C2	139.6 (5)	C1-N1-C2	119.2 (6)
Ni-N2-C11	102.2 (4)	Ni-N2-C12	139.4 (5)	C11-N2-C12	118.4 (5)
Ni-N3-C21	103.5 (4)	Ni-N3-C22	137.5 (5)	C21-N3-C22	119.0 (6)
C1-N4-C4	114.4 (6)	C11-N5-C14	114.5 (6)	C21-N6-C24	115.0 (6)
S1-C1-N4	122.4 (5)	N1-C1-N4	124.1 (6)	N1-C2-C3	119.5 (8)
C2-C3-C4	117.4 (8)	N4-C4-C3	125.2 (8)	S2-C11-N2	112.6 (5)
S2-C11-N5	123.9 (5)	N2-C11-N5	123.5 (6)	N2-C12-C13	121.3 (7)
C12-C13-C1	115.4 (8)	N5-C14-C13	126.8 (8)	S3-C21-N3	113.8 (5)
S3-C21-N6	123.6 (5)	N3-C21-N6	122.7 (6)	N3-C22-C23	120.5 (7)
C22-C23-C2	117.5 (8)	N6-C24-C23	125.3 (8)		

of the anion is shown in Figure 1. Selected bond distances and angles are listed in Table III.

The crystal and molecular structure of **3** closely resembles that of $(Et_4N)[Fe(SC_5H_4N)_3]^{16}$ and was briefly reported as a footnote in a previous paper.^{17a} The coordination geometry around nickel is highly distorted octahedral due to the presence of three four-membered N,S-chelate rings. The N-Ni-S angles lie within a very compact span of 67.4 (1)–67.8 (1)°. The unusually small "bite" of the py2S⁻ ligand has been observed in several metal complexes.^{16,23,24} Two of the three S donor atoms are trans to each other while the third one is trans to a N atom. Thus the unsymmetric bidentate thiolate ligand gives rise to a *mer* isomer.

The Ni(II)-N bond distances in **3** fall in the narrow range of 2.034–2.081 Å (Table III). The Ni-N bond that is trans to a Ni-S bond is the longest probably due to the "trans influence" of the S donor atom. In *trans*-[NiCl₂(py)₄]²⁵ and [Ni(NO₃)₂(H₂O)₂(py)₂]²⁶ the average Ni(II)-N_{py} bond lengths are 2.133 (4) and 2.095 (3) Å, respectively. Whenever the pyridine ring is part of a multidentate ligand, the Ni(II)-N_{py} bond length is shortened. For example, in the pyridine-2-carboxamide complex *trans*-[Ni(H₂O)₂(C₆H₆N₂O)₂]₂Cl₂,²⁷ the Ni(II)-N_{py} distance is 2.02 Å. Several distorted tetrahedral complexes of divalent nickel with arenethiolates are known.⁸⁻¹⁰ The Ni(II)-S_{th} (th = thiolate)

(23) Fletcher, S. R.; Skapski, A. C. *J. Chem. Soc., Dalton Trans.* **1972**, 635.
 (24) Masaki, M.; Matsunami, S.; Veda, H. *Bull. Chem. Soc. Jpn.* **1978**, *51*, 3298.

(25) Long, G. J.; Clarke, P. J. *Inorg. Chem.* **1978**, *17*, 1394.

(26) Cameron, A. F. Taylor, D. W.; Nuttall, R. H. *J. Chem. Soc., Dalton Trans.* **1972**, 422.

(27) Masuko, A.; Nomura, T.; Saito, Y. *Bull. Chem. Soc. Jpn.* **1967**, *40*, 511.

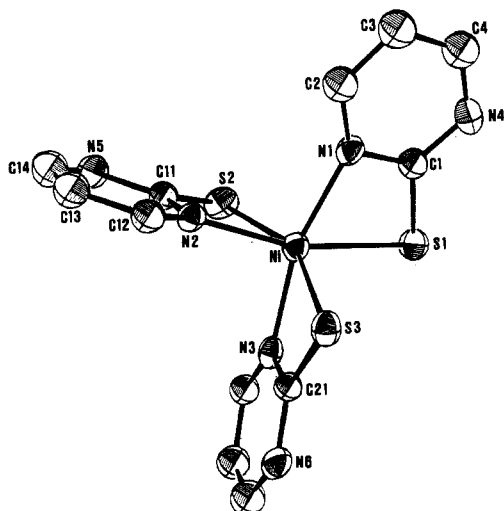


Figure 2. ORTEP drawing of $[\text{Ni}(\text{SC}_4\text{H}_3\text{N}_2)_3]^-$ (anion of **4b**) showing 30% probability ellipsoids and the atom-labeling scheme. Hydrogen atoms are omitted for clarity.

bond lengths in these complexes fall in the range 2.269–2.288 Å. In *cis*-bis(2,2'-bipyridine)bis(benzenethiolato)nickel(II),¹⁵ a rare example of an octahedral complex of Ni(II) containing thiolates as ligands, the Ni(II)–S_{th} bond is 2.445 (2) Å. In **3**, the average Ni(II)–S_{th} distance is 2.528 (1) Å. It is thus clear that both Ni–N and Ni–S bond lengths in **3** are somewhat longer than what are generally observed in analogous compounds. Steric strain in the four-membered chelate rings appears to be primarily responsible for the stretched metal–donor bonds.

Structure of $(\text{Ph}_4\text{P})[\text{Ni}(\text{SC}_4\text{H}_3\text{N}_2)_3]\cdot\text{CH}_3\text{CN}$ (4b**).** This compound also crystallizes in the monoclinic space group $\text{P}2_1/\text{c}$. The structure of the discrete anion is shown in Figure 2. Selected bond distances and angles are collected in Table III.

The coordination structure of nickel in **4b** is very similar to that in **3**. Three four-membered N₂S₂-chelate rings are present, and the geometry around nickel is highly distorted octahedral. The N–Ni–S angles lie in a narrow range of 67.1 (1)–68.3 (2)°. The same kind of small "bite" of the pm2S⁻ ligand has been observed in $(\text{Me}_4\text{N})[\text{Fe}(\text{SC}_4\text{H}_3\text{N}_2)_3]$.¹⁷ The disposition of donor atoms around nickel in **4b** is identical with that found in **3**, and the isolated complex is the *mer* isomer.

In **4b**, the average Ni(II)–N_{pm} (pm = pyrimidine) distance is 2.043 (5) Å. This distance is slightly shorter than the average Ni(II)–N_{py} distance in **3**. At present, no Ni(II)–N_{pm} bond distance is available for comparison. The Ni(II)–N_{pm} distance in **4b** is, however, close to the average Fe(II)–N_{pm} distance of 2.163 (2) Å in $(\text{Me}_4\text{N})[\text{Fe}(\text{SC}_4\text{H}_3\text{N}_2)_3]$.¹⁷ When the Ni(II)–N and Ni(II)–S_{th} distances in the two complexes are compared, it appears that pm2S⁻ is the stronger ligand. Spectroscopic studies also suggest that the crystal field strength of pm2S⁻ is higher than that of py2S⁻ (vide infra). The same trend is observed with the iron(II) complexes.^{16,17} Interesting is to note that in both structures, one chelate ring (ring 1 in **3**, ring 3 in **4b**) consists of a comparatively longer Ni(II)–S_{th} and a shorter Ni(II)–N bond.

Properties

In solid state, the complexes **3–4b** are not sensitive to oxygen. The crystals turn dark only when kept in air for a few weeks. Solutions in acetonitrile and DMF, however, slowly decompose on exposure to air. Thiolato complexes of the type $[\text{Ni}(\text{SAr})_4]^{2-}$ (Ar = arene) are highly susceptible to protic solvents.^{9,10} Thus addition of ca. 10% alcohol to acetonitrile solution of an arene-thiolate causes rapid precipitation of insoluble polymer(s). Contrary to this characteristic, solutions of the present complexes (**3–4b**) are quite stable. Addition of ca. 50% alcohol or even water to solution of these complexes in DMF does not bring about precipitation of any insoluble polymeric material. Also, the electronic spectrum of **4a** in methanol (Table IV) indicates no decomposition over a period of 3–4 h. Complex **3** is comparatively

Table IV. Spectroscopic and Electrochemical Data for $(\text{Et}_4\text{N})[\text{Ni}(\text{SC}_5\text{H}_4\text{N})_3]$ (**3**), $(\text{Et}_4\text{N})[\text{Ni}(\text{SC}_4\text{H}_3\text{N}_2)_3]$ (**4a**), and $(\text{Ph}_4\text{P})[\text{Ni}(\text{SC}_4\text{H}_3\text{N}_2)_3]\cdot\text{CH}_3\text{CN}$ (**4b**)

Electronic Spectrum		
compd	solvent	λ_{max} , nm (ϵ , $\text{M}^{-1}\text{cm}^{-1}$)
3 ^a	MeCN	1150 (24), 975 sh, 620 (35), 284 (39 000)
	DMF	1170 (25), 975 sh, 620 (36), 287 (40 300)
4a	MeCN	1110 (28), 950 sh, 612 (44), 284 (41 500)
	DMF	1130 (30), 950 sh, 610 (44), 287 (43 100)
4b ^b	MeOH	1110 (27), 960 sh, 610 (35), 275 (44 000)
	DMF	1125 (27), 960 sh, 610 (38), 280 (42 000)
	DMF	1130 (26), 950 sh, 610 (41), 287 (41 300)
¹ H NMR Spectrum		
compd	solvent	chem shift, ppm ($\sim 298\text{ K}$)
3	CD_3CN	-98.05, -70.83, -54.50, -12.31
	$\text{DMF}-d_7$	-99.23, -70.55, -54.71, -12.48
4a	CD_3CN	-99.20, -45.95, -15.25
	$\text{DMF}-d_7$	-101.26, -46.34, -15.03
4b ^c	$\text{DMF}-d_7$	-101.20, -46.20, -15.04
Peak Potential for Oxidation ^d		
compd	solvent	E_p , ^e V
3	MeCN	+0.07
	DMF	+0.16
4a	MeCN	+0.32
	DMF	+0.46

^a Complex decomposes in MeOH. ^b Not sufficiently soluble in MeOH. ^c Not sufficiently soluble in CD_3CN . ^d Cyclic voltammetry and differential-pulse polarography (dpp), Pt-inlay electrode, 0.1 M tetrabutylammonium perchlorate as supporting electrolyte, and 50 mV/s scan speed; for dpp, modulation 25 mV peak to peak, 5 mV/s scan speed, and clock 0.5 s. ^e Values quoted vs. aqueous SCE.

less stable in protic solvents and decomposes in 2:1 v/v MeOH/DMF mixture. The extra stability of the present complexes toward protic solvents might arise from additional donor groups in the thiolate ligands.

Absorption Spectra. Electronic absorption spectra for **3** and **4a** are shown in Figure 3, and the spectral parameters are collected in Table IV. In octahedral and pseudooctahedral Ni(II) (d^8) complexes, the three spin-allowed transitions from ${}^3A_{2g}$ to ${}^3T_{2g}$, ${}^3T_{1g}$, and ${}^3T_{1g}(\text{P})$ generally fall within the ranges 1430–770, 910–500, and 530–370 nm, respectively, with intensities less than $30\text{ M}^{-1}\text{cm}^{-1}$ in regular octahedral systems.²⁸ The crystal field around nickel in **3–4b** is highly distorted, and the deviation from octahedral symmetry is reflected in (a) larger values for the extinction coefficients (Table IV) and (b) the double-humped absorption band for the ${}^3A_{2g} \rightarrow {}^3T_{2g}$ transition (Figure 3). If we take the energy of the midpoint of the double-humped band as $10Dq$, it appears that both the thiolates are weak ligands for Ni(II). In case of the Fe(II) complexes,^{16,17} variable-temperature Mossbauer data in the polycrystalline state and the blue shift of the absorption maxima in solution suggest that between these two thiolates, pm2S⁻ is the stronger donor to divalent iron center. The same trend is observed with Ni(II) in the present work. The ${}^3A_{2g} \rightarrow {}^3T_{2g}$ transition in **4a** and **4b** is blue-shifted compared to that in **3** (Table IV, Figure 3). The second spin-allowed ${}^3A_{2g} \rightarrow {}^3T_{1g}$ transition in **3–4b** gives rise to a narrow band in the region of 600–650 nm.

¹H NMR Spectra. The various peak positions are listed in Table IV and spectra for **3** and **4b** in $(\text{CD}_3)_2\text{NCDO}$ ($\text{DMF}-d_7$) are shown in Figure 4. Unlike the tetrahedral thiolato complexes $[\text{Ni}(\text{SAr})_4]^{2-}$, which give rise to sharp resonances for the thiolato protons,¹⁰ complexes **3–4b** exhibit broad resonances over a greater spread of chemical shift (Figure 4). The half-height widths of the NMR peaks in CD_3CN are somewhat smaller than those in $(\text{CD}_3)_2\text{NCDO}$. Assignment of the broad and contact-shifted peaks has not been completed at the present time.

(28) Lever, A. B. P. In *Inorganic Electronic Spectroscopy*, 2nd ed.; Elsevier: Amsterdam, 1984; p 507.

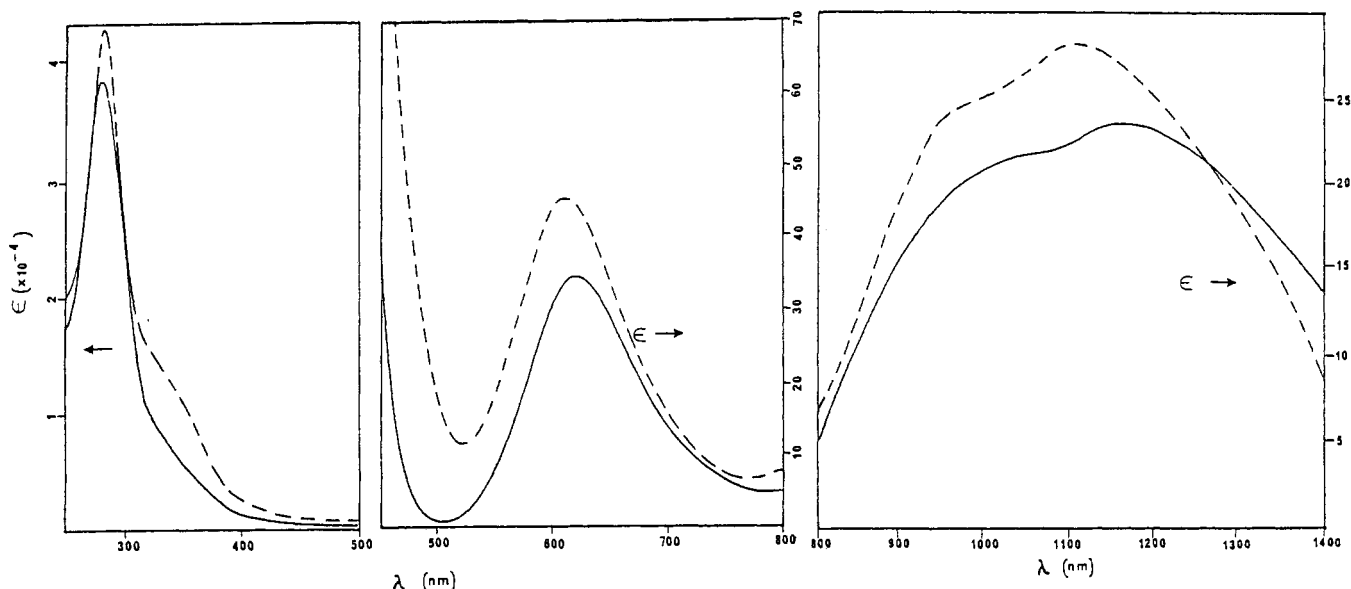


Figure 3. Absorption spectra of **3** (solid line) and **4a** (broken line) in MeCN solution (ϵ values are in units of $M^{-1} \text{ cm}^{-1}$).

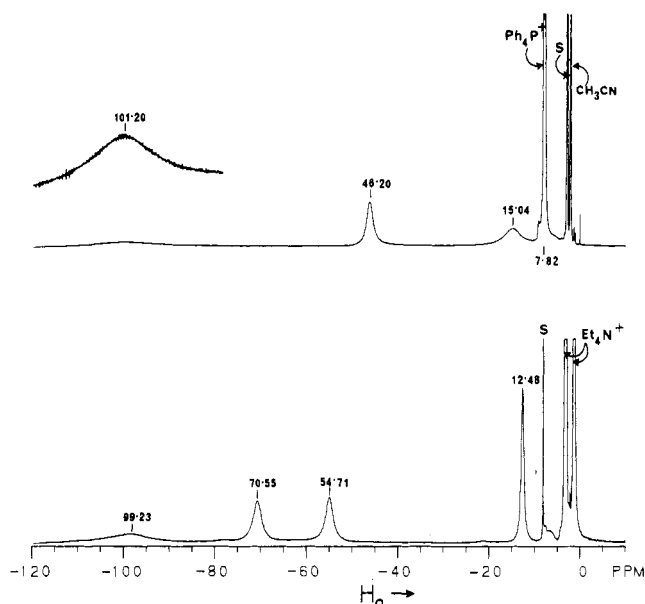


Figure 4. ^1H NMR spectra (300 MHz, 298 K) of $(\text{Et}_4\text{N})[\text{Ni}(\text{SC}_4\text{H}_4\text{N})_3]$ (**3**, lower) and $(\text{Ph}_4\text{P})[\text{Ni}(\text{SC}_4\text{H}_3\text{N}_2)_3] \cdot \text{CH}_3\text{CN}$ (**4b**, upper) in $\text{DMF}-d_7$. S = Solvent peak; in both spectra one or two S peaks are hidden under the cation resonance.

Redox Properties. In acetonitrile and DMF, the nickel complexes **3–4b** undergo irreversible oxidation. Peak potentials for such oxidation are collected in Table IV. Cyclic voltammetric studies indicate that the oxidized species undergo rapid chemical decomposition near the working electrode since no current response is noted in the reverse scan. Electrochemical behavior is identical on both glassy-carbon and Pt electrodes. In DMF, **4a** exhibits a relatively clean differential-pulse polarogram for the process

of oxidation though the half-height width (140 mV) is much larger than the value (90 mV) for a reversible system. Spectroscopic studies indicate that in divalent nickel complexes, the ligand field strength of $\text{pm}2\text{S}^-$ is higher than of $\text{py}2\text{S}^-$. Electrochemical studies suggest that $\text{pm}2\text{S}^-$ also gives rise to a Ni(II) complex (**4a**) that is more resistant to oxidation.

Summary

The following are the principal results and conclusions of this investigation.

(1) Two new discrete thiolato complexes of divalent nickel $[\text{Ni}(\text{S}2\text{py})_3]^-$ (**3**) and $[\text{Ni}(\text{S}2\text{pm})_3]^-$ (**4a**, **4b**) have been isolated. These species belong to a relatively scarce class of octahedral nickel(II) complexes that contain thiolato S donor atoms.

(2) The crystal structure of **3** and **4b** reveal the presence of three four-membered N,S-chelate rings with N–Ni–S bite angles close to 67° . The coordination geometry around nickel is distorted octahedral, and the isolated complexes are *mer* isomers.

(3) Unlike the tetrahedral thiolato complexes $[\text{Ni}(\text{SAr})_4]^{2-}$, these octahedral species are stable in the presence of protic solvents like alcohols.

Acknowledgment. This research was supported by a Faculty Research Committee Grant and the donors of the Petroleum Research Fund, administered by the American Chemical Society, at the University of California, Santa Cruz, CA. D.W.S. acknowledges financial support from the NSERC of Canada. L.G. and H.P.B. are recipients of NSERC scholarships.

Registry No. **3**, 109364-43-4; **4a**, 109364-45-6; **4b**, 109364-47-8.

Supplementary Material Available: Thermal parameters for non-hydrogen atoms (Table S1), hydrogen atom parameters (Table S2), and bond distances and angles associated with the cations and the acetonitrile molecule (Table S3) for $(\text{Et}_4\text{N})[\text{Ni}(\text{SC}_4\text{H}_4\text{N})_3]$ (**3**) and $(\text{Ph}_4\text{P})[\text{Ni}(\text{SC}_4\text{H}_3\text{N}_2)_3] \cdot \text{CH}_3\text{CN}$ (**4b**) (7 pages); values of $10|F_o|$ and $10|F_c|$ (Table S4) (20 pages). Ordering information is given on any current masthead page.